Food & Function

ROYAL SOCIETY OF CHEMISTRY

PAPER

View Article Online
View Journal | View Issue

Cite this: *Food Funct.*, 2025, **16**, 5151

Preventive and controlling effects of *N*-acetylneuraminic acid in regulating glucose and lipid metabolism disorders *via* the gut-liver axis in high-fat diet mice

Wei Zhang,†[a,b] Linlin Zhou,†[a,b] Xinyuan Huang,[a,b] Xinning Zhao,[a,b] Hanying Zheng,[a,b] Dongbei Guo,[a,b] Xiaoxuan Chen,[a,b] Lili Pan,[a,b] Yahui Li*[c,d,e,f] and Hongwei Li *[a,b]

A high-fat diet may disrupt sialic acid homeostasis indirectly by altering the gut microbiota and metabolic pathways. Sialic acid interventions have immune-regulatory effects and can improve gut health, but their impact on glucose and lipid metabolism disorders, both before and after obesity induced by a high-fat diet, remains unclear. This study used two models: a preventive experiment (intervention during high-fat diet feeding) and a control experiment (intervention after obesity induction). Each model consisted of a blank control group, a high-fat diet control group, and three *N*-acetylneuraminic acid (Neu5Ac) intervention groups (low, medium, and high doses), with 12 mice per group. The results showed that both intervention models effectively improved glucose tolerance, and reduced insulin levels, although no significant dose–response relationship was observed. Omics analysis revealed that the intervention increased the abundance of gut microbiota associated with energy metabolism and affected energy metabolism, immune response, and oxidative stress-related signaling pathways in the liver and colon. In the control experiment, inflammation marker levels correlated with improvements in the gut microbiota. Furthermore, the intervention significantly altered the abundance of microbiota linked to glycosylation signaling and metabolic regulation. These findings suggest that Neu5Ac intervention improves gut microbiota structure and function, stabilizes glycan structures, and reduces immune-inflammatory signaling in the gut and liver, thereby lowering systemic inflammation. This helps prevent and control glucose and lipid metabolism disorders induced by a high-fat diet. Notably, the intervention showed stronger effects after obesity had developed due to the high-fat diet.

Received 24th January 2025,
Accepted 23rd May 2025

DOI: 10.1039/d5fo00484e

rsc.li/food-function

1. Introduction

Rapid advancements in food manufacturing have significantly altered human lifestyles and dietary habits, particularly contributing to the rising prevalence of high-fat diets (HFDs).[1,2] Extensive research has shown that long-term HFD consumption can lead to a variety of pathological conditions, including organ fat accumulation, dysbiosis of the gut microbiota, insulin resistance, colon damage, oxidative stress, and cognitive impairment.[3–6] Chronic diseases linked to long-term HFD consumption include obesity, diabetes, gastrointestinal disorders, neurodegenerative diseases, and cardiovascular diseases.[4,7–9] Obesity has become a global health crisis, with its rising prevalence posing significant public health challenges. According to the World Health Organization, approximately 500 million individuals are obese, and 1.4 billion are overweight, with both numbers continuing to increase. This trend has a profound impact on public health and daily life.[10]

In promoting the onset and progression of obesity, a high-fat diet not only disrupts glucose and lipid metabolism and affects insulin sensitivity but also activates immune cells in the small intestine. This activation leads to mucosal immunity, triggers systemic immunosuppression and inflammatory responses, and reduces the immunity of antigen-specific CD4+ T cells.[11] Recent studies have revealed a close relationship

[a]*State Key Laboratory of Vaccines for Infectious Diseases, Xiang An Biomedicine Laboratory, School of Public Health, Xiamen University, China.*
E-mail: rocque@xmu.edu.cn; Fax: +0086-0592-2181578; Tel: +86-18905920451
[b]*State Key Laboratory of Molecular Vaccinology and Molecular Diagnostics, National Innovation Platform for Industry-Education Integration in Vaccine Research, Xiamen University, China*
[c]*State Key Laboratory of Food Science and resources, Jiangnan University, Wuxi, Jiangsu 214122, China. E-mail: 2269380010@qq.com*
[d]*School of Food Science and Technology, Jiangnan University, Wuxi, Jiangsu 214122, China*
[e]*National Engineering Research Center for Functional Food, Jiangnan University, Wuxi, Jiangsu 214122, China*
[f]*Wuxi Institute for Specialized Nutrition and Health Co., Ltd, Wuxi, Jiangsu 214122, China*
†These authors contributed equally to this study.

between food composition and changes in the gut microbiota, which significantly impacts host metabolic regulation.[12–14] The gut microbiota is strongly linked to the host's immune system and energy metabolism.[15] Imbalances in the gut microbiota are considered a key environmental factor in various metabolic and chronic diseases. A high-fat diet can alter the gut microbiota, leading to the production of pathogenic factors that affect liver function. These factors can activate immune cells, causing inflammation and even fibrosis in the liver through the gut-liver axis.[16] Therefore, interventions aimed at improving gut microbiota balance, reducing inflammation, and modulating immune responses to control glucose and lipid metabolism disorders in individuals on high-fat diets may be effective strategies for preventing obesity.[17,18]

In recent years, sialic acid has garnered significant attention in the search for effective ways to prevent and control glucose and lipid metabolism disorders caused by high-fat diets. Its potential role in gut health and immune regulation has made it a key research focus. Sialic acid, scientifically known as *N*-acetylneuraminic acid (Neu5Ac), is a nine-carbon glyconeuraminic acid that possesses antioxidant,[19] immune-modulating,[20] antiviral,[21] intestinal microbiota-regulating[22] and antitumor effects.[23] Countries such as China, the European Union, Japan, Malaysia, and Singapore have already incorporated Neu5Ac as a food ingredient. As a crucial molecule in immune signaling and cell-to-cell communication, sialic acid plays a vital role in immune responses. Although direct evidence linking high-fat diets to sialic acid hydrolysis from glycolipids or glycoproteins is lacking, studies suggest that metabolites such as bile acids, lipopolysaccharides, short-chain fatty acids, and trimethylamine oxide may be involved in the pathogenesis of high-fat diets and chronic diseases. These metabolites may indirectly influence sialic acid levels. Disturbances in the gut microbiota, in turn, can affect metabolic processes throughout the body, possibly including the metabolism of sialic acid.[3] Therefore, high-fat diets may indirectly disrupt sialic acid homeostasis by affecting the gut microbiota and metabolic pathways, resembling the disruptions caused by high-fat diets themselves. Furthermore, animal and cell experiments have demonstrated that sialic acid intervention activates immune cells and modulates immune responses, with a dose–response relationship.[24,25]

Recent studies have shown that high-fat diets can alter the synthesis and metabolism of sialic acid, disrupt the gut microbiota, impair immune homeostasis, and increase susceptibility to inflammatory diseases. Neu5Ac intervention has been found to improve the sialylation status in the body.[26] Based on this, we hypothesize that restoring sialic acid modification may positively influence the structure and function of the gut microbiota, maintain immune homeostasis in both the intestine and liver, reduce systemic inflammation, and improve glucose and lipid metabolism. These effects could potentially mitigate metabolic disorders associated with glucose and lipid metabolism. To test this hypothesis, we designed two models —prevention and control—to evaluate the effects of sialic acid intervention. In the prevention model, sialic acid is administered alongside a high-fat diet, which may slow the degradation of sialic acid and mitigate gut microbiota disruption, ultimately preventing glucose and lipid metabolism disorders induced by the high-fat diet. In the control model, we observe whether sialic acid intervention can alleviate microbiota imbalances, immune dysfunction, and chronic inflammation in the obese state, potentially hindering the progression of obesity. We will compare the two models in terms of intestinal microbiota, intestinal barrier, intestinal immunity, and gut-liver axis signaling, using transcriptomics and metabolomics techniques. This approach aims to provide a comprehensive understanding of the effects of sialic acid intervention on the prevention and control of glucose and lipid metabolism disorders, and even obesity, which may be induced by immune signal disruption caused by a high-fat diet.

2. Materials and methods

2.1 Source of materials

N-Acetylneuraminic acid (Neu5Ac) [specification: ≥98% high-performance liquid chromatography (HPLC)] was provided by Wuhan CASOV Green Biotech Co., Ltd (China).

2.2 Animal experiments and ethical approval statement

6-Week-old male C57BL/6J mice were purchased from Beijing Witte River Laboratory Animal Co., Ltd.

In the prevention model experiment, 60 male C57BL/6J mice were housed at 20–24 °C, humidity 10–60%, and light–dark cycle for 12 h. Twelve mice were selected according to the immediate number method and fed with normal diet (ND) [Beijing Gaoxieli Feed Co., Ltd; Beijing Feed Certificate (2018), 0673]. The remaining 48 mice were fed a high-fat diet [Research Diets, Inc., D12492; Jiangsu Shuangshi Laboratory Animal Feed Department, Su Feed Certificate (2017) 05005], in which the fat ratio was 60%, and it was divided into 4 groups, namely high-fat feed group (HFD) and 3 intervention groups: low-dose (Neu5Ac_L1), medium-dose (Neu5Ac_M1), and high-dose (Neu5Ac_H1) group (Table 1).

In the control model experiment, based on our previous experience, the success rate of the high-fat diet-fed obesity model was 40%. After 1 week of acclimatization, 12 male mice (n = 132) were selected to continue to be fed a normal diet (ND) for 8 weeks. The remaining 120 mice were fed a high-fat diet [Research Diets, Inc., D12492; Jiangsu Shuangshi Laboratory Animal Feed Department, Su Feed Certificate (2017) 05005], fat accounts for 60% of calories. Mice with a 40% increase in body weight after feeding with high-fat diet were screened as successful obesity models, and 48 obese mice were screened and randomly divided into 1 model control (HFD_2) and 3 intervention groups, namely low-dose (Neu5Ac_L2), medium-dose (Neu5Ac_M2), and high-dose (Neu5Ac_H2) groups, with 12 mice in each group.

In the experiment, the dosage of the Neu5Ac_M group was calculated according to the recommended human intake of

Table 1 Animal experimental protocol

Experiment	Group	*N*	Test substance	Supplementation dose in mice (mg d^{-1} kg^{-1})	Gavage concentration (mg mL^{-1})
Preventive	Normal diet (ND_1)	12	Normal saline	—	—
	High fat diet group (HFD_1)		Normal saline	—	—
	Neu5Ac_L1	12	*N*-Acetylneuraminic acid	50	5.00
	Neu5Ac_M1	12	*N*-Acetylneuraminic acid	100	10.00
	Neu5Ac_H1	12	*N*-Acetylneuraminic acid	150	15.00
Control	Normal diet (ND_2)	12	Normal saline	—	
	High fat diet group (HFD_2)	12	Normal saline		
	Neu5Ac_L2	12	*N*-Acetylneuraminic acid	50	5.00
	Neu5Ac_M2	12	*N*-Acetylneuraminic acid	100	10.00
	Neu5Ac_M2	12	*N*-Acetylneuraminic acid	150	15.00

bird's nest (3 g d^{-1}),[27] in which the Neu5Ac content was 10%.[28] The gavage dose in the Neu5Ac_M group was 10 times the recommended dose for human and animal surface area, *i.e.*, the gavage dose in the Neu5Ac_M group was 50.0 mg d^{-1} kg^{-1}. The dose administered to the Neu5Ac_L group was 50% of that of the Neu5Ac_M group, and the dose administered to the Neu5Ac_H group was twice that of the Neu5Ac_M group. The dose of Neu5Ac is similar to that of previous studies.[29] The ND group and HFD group were given 0.9% normal saline in a volume of 0.1 mL per 10 g body weight. Weekly body weight and food intake were measured by gavage in mice with a gavage volume of 0.1 mL per 10 g of mouse body weight. The intervention period of preventive experiment was 8 weeks. The intervention period of control experiment was 10 weeks.

At the end of the intervention, fasting blood glucose (FBG) and glucose tolerance (OGTT) were tested at the end of the intervention, and the mice were given 20% glucose solution according to their body weight (10 μL g^{-1}) immediately after fasting for 12 h. At 0, 30, 60 and 120 min after glucose administration, blood is taken from the tail vein of mice, and blood glucose concentrations are measured using a blood glucose meter (Sinocare Biosensing Co., Ltd). Fat mass and lean mass of mice are analyzed using the EchoMRI-100 h instrument (EchoMRI International Medical Devices, Inc.).

All experimental procedures were carried out in accordance with the guidelines of the Institutional Animal Care and Use Committee of the Laboratory Animal Center of Xiamen University and the International Association of Veterinary Editors guidelines for the Care and Use of Laboratory Animals. Protocols for animal use were reviewed and approved by the Animal Ethical and Welfare Committee of the Laboratory Animal Center of Xiamen University (Approval No. XMULAC 20210010).

2.3 Sample collecting and index testing

When the intervention ended, the mice fasted for 12 h, were anaesthetised with 4% isoflurane (Shenzhen Reward Life Technology Co., Ltd) and then euthanised through rapid spinal dislocation. Blood was collected from mice *via* retro-orbital bleeding under anesthesia. Organs (liver, colon, and the content of colon) and fat [perirenal fat[30] (refers to the fat surrounding the kidneys in mice (peri-renal adipose tissue)), peritesticular fat[31] (refers to the fat surrounding the testes and associated structures (*e.g.*, epididymis, spermatic cord) in mice), and mesenteric fat[32] (dissected from the jejunoileal mesentery following vascular landmarks)] were collected, rinsed with 0.9% saline, and the fat weighed rapidly. The collected blood was centrifuged at 2000 rpm at 4 °C for 15 min, and the resultant supernatant was collected to measure biochemical indicators. All samples were frozen at −80 °C for later use.

2.4 Serum biochemical indicators

The aspartate aminotransferase (AST), alanine aminotransferase (ALT), total cholesterol (TC), triglycerides (TG), high-density lipoproteins (HDL), and low-density lipoproteins (LDL) in serum were detected by an automatic biochemical analyser (Mindray BS-220) and a special kit. The insulin (INS), lipopolysaccharide (LPS), oxidized low-density lipoprotein (OX-LDL), trimethylamine *N*-oxide (TMAO), glucagon-like peptide-1 (GLP-1), interleukin-1β (IL-1β), interleukin-6 (IL-6), and tumor necrosis factor-α (TNF-α) in serum were measured using mouse enzyme-linked immunosorbent assay kits (Shanghai Sanyan Biotechnology Center), according to the manufacturer's instructions.

2.5 Oil red O staining and hematoxylin and eosin (H&E) staining of liver tissue

The liver tissue samples were fixed using 4% paraformaldehyde, paraffin-embedded, cut into sections. Oil red oxygen dyeing was performed with the modified oil red oxygen staining kit (Solarbio Life Sciences, Beijing, China), following the instruction provided by the manufacturer. Hematoxylin–eosin (HE) staining was performed using HE staining kit (Solarbio); stains were then assessed *via* microscopy (Leica-DM4B, Germany).

2.6 16S rDNA sequencing

The content of colon was swiftly frozen in liquid nitrogen post-sampling and stored at −80 °C. DNA was extracted from these samples using the HiPure Stool DNA kit (Magen, Guangzhou, China). The conserved 16S rDNA gene region (V3: 341F, CCTACGGGNGGCWGCAG; V4: 806F, GGACTACHVGGGTATCTAAT) was polymerase chain reaction (PCR)-amplified using suitable primers with barcodes. The

resulting amplicons were purified, quantified, and subjected to equimolar pooling for paired-end sequencing (PE250) on an Illumina sequencer (Life Technologies, CA, USA). Raw reads were filtered, assembled, and processed using FASTP (v. 0.18.0). Clean tags were clustered into operational taxonomic units (OTUs) with a ≥97% similarity threshold using the UPARSE pipeline (v. 9.2.64). Chimeric tags were removed using the UCHIME algorithm, and the remaining tags underwent downstream analyses. The most abundant sequence in each OTU served as a representative sequence. Following OTU determination, the gut microbiota indices were assessed using the Omicsmart platform (Gene Denovo Biotechnology Co., Ltd Guangzhou, China; https://www.omicsmart.com).

2.7 Liver and colon transcriptomic analysis

RNA extraction, construction of a sequencing library, and transcriptome sequencing were carried out by Gene Denovo Biotechnology Co. (Guangzhou, China). A trizol reagent kit (Invitrogen, Carlsbad, CA, USA) was used to extract the total RNA. The quality of RNA was assessed using an Agilent 2100 Bioanalyzer (Agilent Technologies, Palo Alto, CA, USA) and checked using RNase-free agarose gel electrophoresis. After mRNA was reverse transcribed into cDNA, the double-stranded cDNA fragment was connected to the Illumina sequencing connector. Then, they were purified with AMPure XP beads (Beckman, Agencourt, USA) and amplified using polymerase chain reaction (PCR), and the obtained library was commercially sequenced using Illumina Novaseq 6000 sequencer. Fastp[33] (version 0.18.0) was used to further filter high-quality clean reads and remove reads containing connectors, reads containing more than 10% unknown nucleotides, and low-quality reads containing more than 50% of low-quality (Q-value ≤20) bases. The reading fragments were mapped to the ribosomal RNA database by using the short reads alignment tool Bowtie (version 2.2.8).[34] An index of the reference genome was constructed, and pairs of clean terminal reads were mapped to the reference genome using HISAT2. 2.4. Other parameters were set as default values. The mapped reads of each sample were assembled with a reference-based method using StringTie v1.3.1. Principal component analysis (PCA) was performed using the R package gmodels [R: The R Project for Statistical Computing (r-project.org)]. Gene Set Enrichment Analysis (GSEA) analysis is used for the differential genes of the whole data. The Kyoto Encyclopedia of Genes and Genomes (KEGG) enrichment and the Gene Ontology (GO) enrichment analysis were used to explore biological functions in depth.

2.8 Statistical analysis

Data were analyzed using SPSS 22.0 and R statistical software. Repeated measures data were analyzed for variance using multivariate analysis. For normally distributed data with homogeneous variance, a one-way analysis of variance (one-way ANOVA) was used to compare differences between groups, and Fisher's least significant difference method (LSD) was used for pairwise comparisons between groups. In the case of normally distributed data for which the variance was nonhomogeneous, we used Dunnett's T3 test for pairwise comparisons between the groups. For non-normally distributed data, we used the non-parametric Kruskal–Wallis H test for comparison between groups, and the Nemenyi method was used for pairwise comparison of the overall means between groups. For categorical data comparisons (*e.g.*, obesity rates across groups), Chi-square test was applied if ≥80% of cells in the contingency table had expected frequencies ≥5, and no cell had an expected frequency <1, Fisher's exact test was used when the above criteria were not met. Differences were considered significant at the $a = 0.05$ level.

3. Results

3.1 Weight and food energy intake

As shown in Fig. 1(A and B), in the preventive experiment, the body weight of mice in all groups was similar at week 0 ($P > 0.05$). After 8 weeks of intervention, under the condition of no statistically significant difference in food energy intake ($P > 0.05$), no statistically significant differences in body weights were observed between the intervention groups and the HFD group ($P > 0.05$), and no dose-dependent effect was detected. A statistically significant difference in obesity rates was observed across the groups ($\chi^2 = 9.011$, d$f = 3$, $P = 0.029$). The obesity rates in the intervention groups were significantly lower than those in the high-fat diet control group ($P < 0.05$), the detail was showed in Fig. 1(C).

As showed in Fig. 1(D and E), in the control experiment, the body weights of the modeled mice were 29.87 ± 0.84 g (*vs.* ND group 25.66 ± 1.04 g, $P < 0.05$) after modeling. No statistically significant differences in food energy intake were observed between the intervention groups and the HFD_2 group during the intervention period ($P > 0.05$). After 10 weeks of intervention, Neu5Ac_M2 group exhibiting the lowest weight gain rate, significantly lower than that of the HFD_2 group ($P < 0.05$), the detail was showed in Fig. 1(F).

3.2 Fat mass, lean mass and perivisceral fat

As shown in Fig. 2(A), in the preventive experiment, after 8 weeks of intervention, the total fat mass in all intervention groups was significantly lower than that in the HFD_1 group ($P < 0.05$), indicating that sialic acid intervention effectively reduced fat accumulation caused by a high-fat diet. The lean tissue content in the Neu5Ac_M1 group was significantly higher than that in the HFD_1 group ($P < 0.05$) [Fig. 2(B)]. The weights of epididymal fat, perirenal fat, and mesenteric fat were similar across all groups ($P > 0.05$), the detail was showed in Fig. 2(C–E).

In the control experiment, the total fat mass in the Neu5Ac_M2 group was significantly lower than that in the HFD_2 group ($P < 0.05$) [Fig. 2(F)], and its lean tissue weight was significantly higher ($P < 0.05$). No statistically significant differences were observed between other intervention groups and the HFD_2 group ($P > 0.05$) [Fig. 2(G)]. Fat weight measurements for different organs revealed that – peritesticular fat and

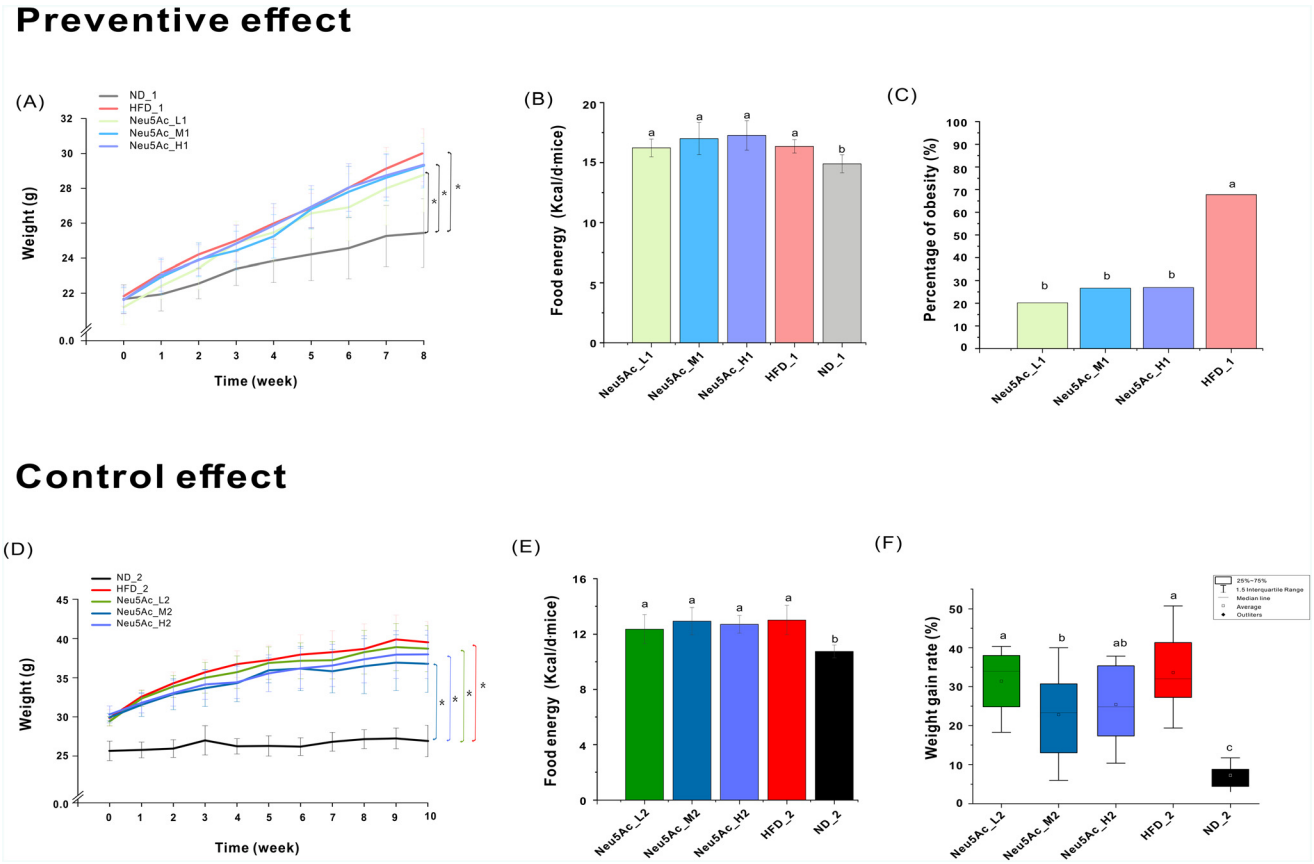

Fig. 1 Effects of *N*-acetylneuraminic acid intervention on body weight and energy intake in high fat-diet mice. (A–C) Preventive experiment: (A) changes in body weight from weeks 0 to 10 of the intervention. Note: * denotes statistically significant differences between groups; (B) average daily food energy intake per mouse; (C) percentage of obesity; (D–F) control experiment: (D) changes in body weight from weeks 0 to 10 of the intervention. Note: * denotes statistically significant differences between groups; (E) average daily food energy intake per mouse; (F) weight gain rate. The difference between values with completely different superscripts was statistically significant, $P < 0.05$. Data are means ± SD ($n = 12$).

mesenteric fat in the Neu5Ac_M2 group were significantly lower than those in the HFD_2 group ($P < 0.05$), the detail was showed in Fig. 2(H and I).

3.3 Fasting blood glucose and OGTT test

As shown in Fig. 3(A), in the prevention experiment, compared to the HFD group, the FBG levels in all intervention groups were significantly lower than those in the HFD_1 group ($P < 0.05$). The changes in the OGTT curve and the comparison of the areas under the curve indicated that, compared to the HFD_1 group, the intervention groups had better glucose tolerance ($P < 0.05$), but still worse than the ND_1 group, with no significant dose–response relationship observed, the detail was showed in Fig. 3(B and C). The insulin levels in the Neu5Ac_M1 group were significantly lower than those in the HFD_1 group ($P < 0.05$), the detail was showed in Fig. 3(D).

As shown in Fig. 3(E), in the control experiment, the FBG levels in the Neu5Ac_M2 and Neu5Ac_H2 groups were lower than those in the HFD_2 group ($P < 0.05$). The changes in the OGTT curve and the comparison of the areas under the curve showed that the intervention groups had better glucose tolerance than the HFD_2 group, with no significant dose–response relationship observed, the detail was showed in Fig. 3(F and G). The insulin levels in the Neu5Ac_M2 group were significantly lower than those in the HFD_2 group ($P < 0.05$), the detail was showed in Fig. 3(H).

3.4 Blood lipids and serum inflammatory cytokine

Whether in the prevention or control experiment, the results of body weight, body fat, and blood glucose all showed no significant dose–response relationship for the intervention effects of Neu5Ac in the three dosage groups. The medium-dose group was selected as a representative for comparing blood lipid levels and serum inflammatory cytokine.

As shown in Fig. 4(A–D), in the prevention experiment, the TG, TC, and LDL levels in the Neu5Ac_M1 group showed no statistically significant differences compared to those in the HFD_1 group. However, HDL was higher in the Neu5Ac_M1 group compared to the HFD_1 group ($P < 0.05$). As shown in Fig. 4(E–H), serum inflammatory cytokines (IL-1β, IL-6, and TNF-α) in the Neu5Ac_M1 group were no significantly lower than those in the HFD_1 group (all $P > 0.05$), while serum GLP-1 levels were higher than in the HFD_1 group ($P < 0.05$).

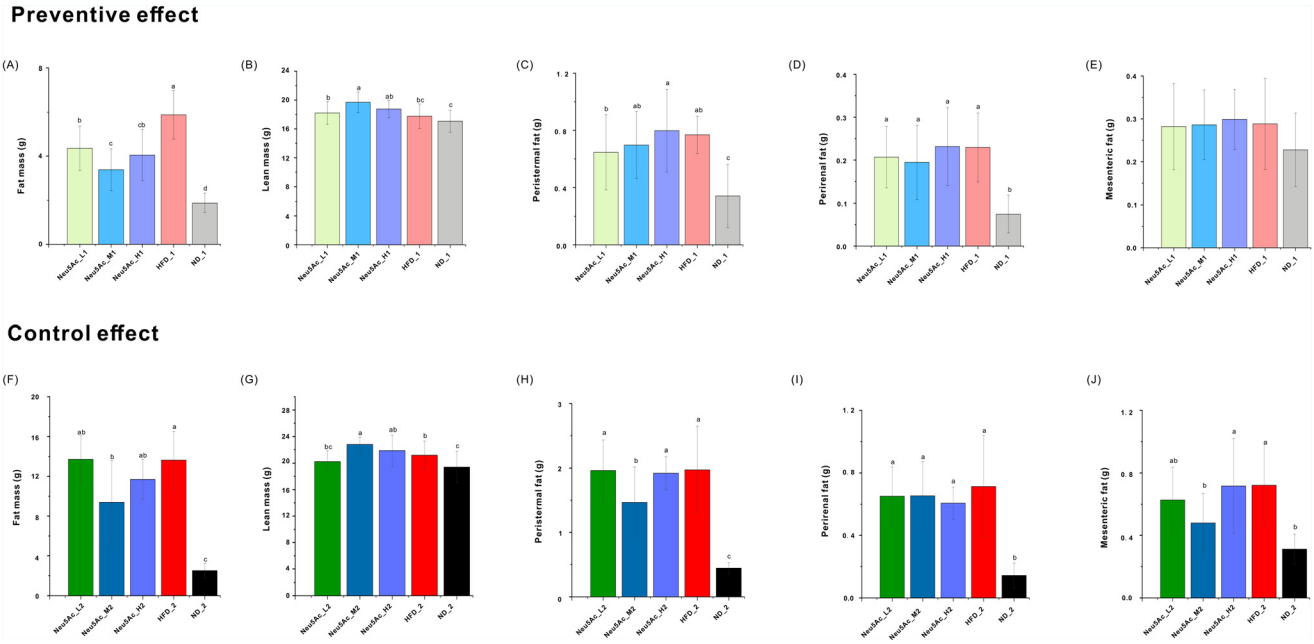

Fig. 2 Effects of *N*-acetylneuraminic acid intervention on fat mass, peri-organ fat content and lean mass in high fat-diet mice. (A–E) Preventive experiment: (A) fat mass; (B) lean mass; (C) peristermal fat weight; (D) perirenal fat weight; (E) mesenteric fat weight; (F–J) control experiment: (F) fat mass; (G) lean mass; (H) peristermal fat weight; (I) perirenal fat weight; (J) mesenteric fat weight. The difference between values with completely different superscripts was statistically significant, $P < 0.05$. Data are means ± SD ($n = 12$).

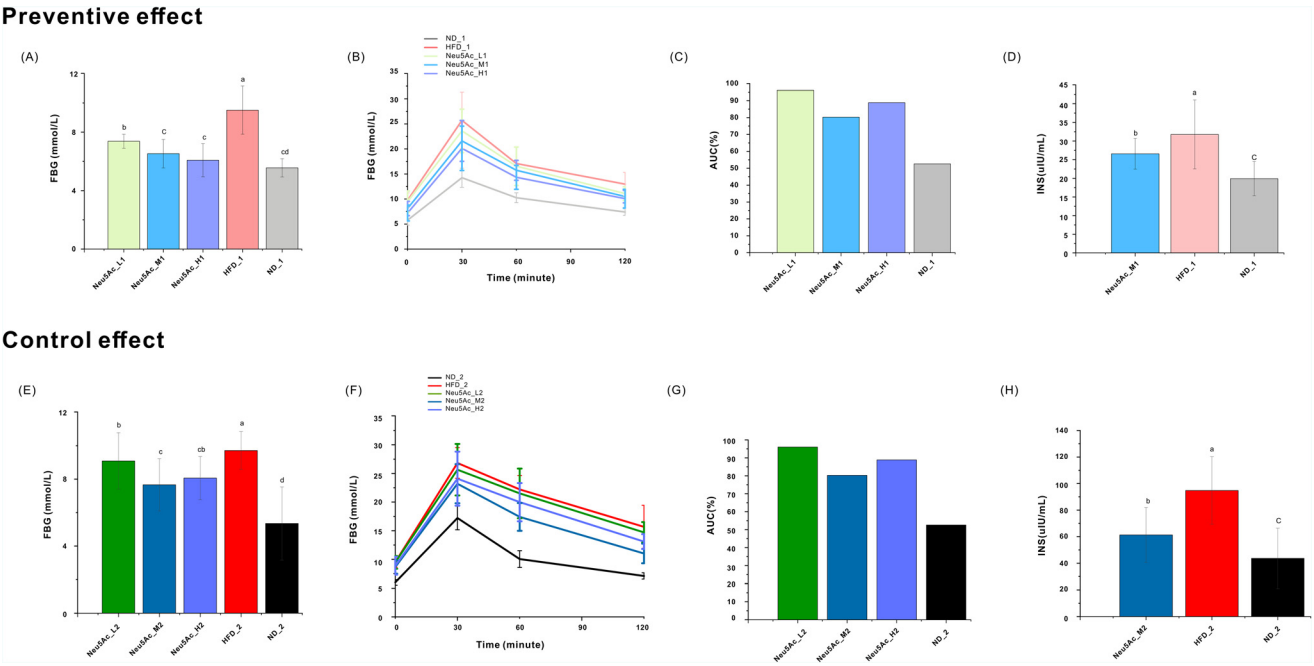

Fig. 3 Effects of *N*-acetylneuraminic acid intervention on blood glucose levels and glucose regulation in high fat-diet mice. (A–D) Preventive experiment: (A) FBG (fasting blood glucose); (B) OGTT (oral glucose tolerance tests); (C) the relative value of the area under the OGTT curve (with the HFD group as the reference); (D) INS (insulin in sera); (E–H) control experiment: (E) FBG (fasting blood glucose); (F) OGTT (oral glucose tolerance tests); (G) the relative value of the area under the OGTT curve (with the HFD group as the reference); (H) INS (insulin in sera). The difference between values with completely different superscripts was statistically significant, $P < 0.05$. Data are means ± SD ($n = 12$).

As shown in Fig. 4(I–L), in the control experiment, the TG, TC, and LDL levels in the Neu5Ac_M2 group were lower than those in the HFD_2 group ($P < 0.05$), and HDL was higher than in the HFD_2 group ($P < 0.05$). As shown in Fig. 4(M–P), serum inflammatory cytokines (IL-1β, IL-6, and TNF-α) in the Neu5Ac_M2 group were significantly lower than those in the

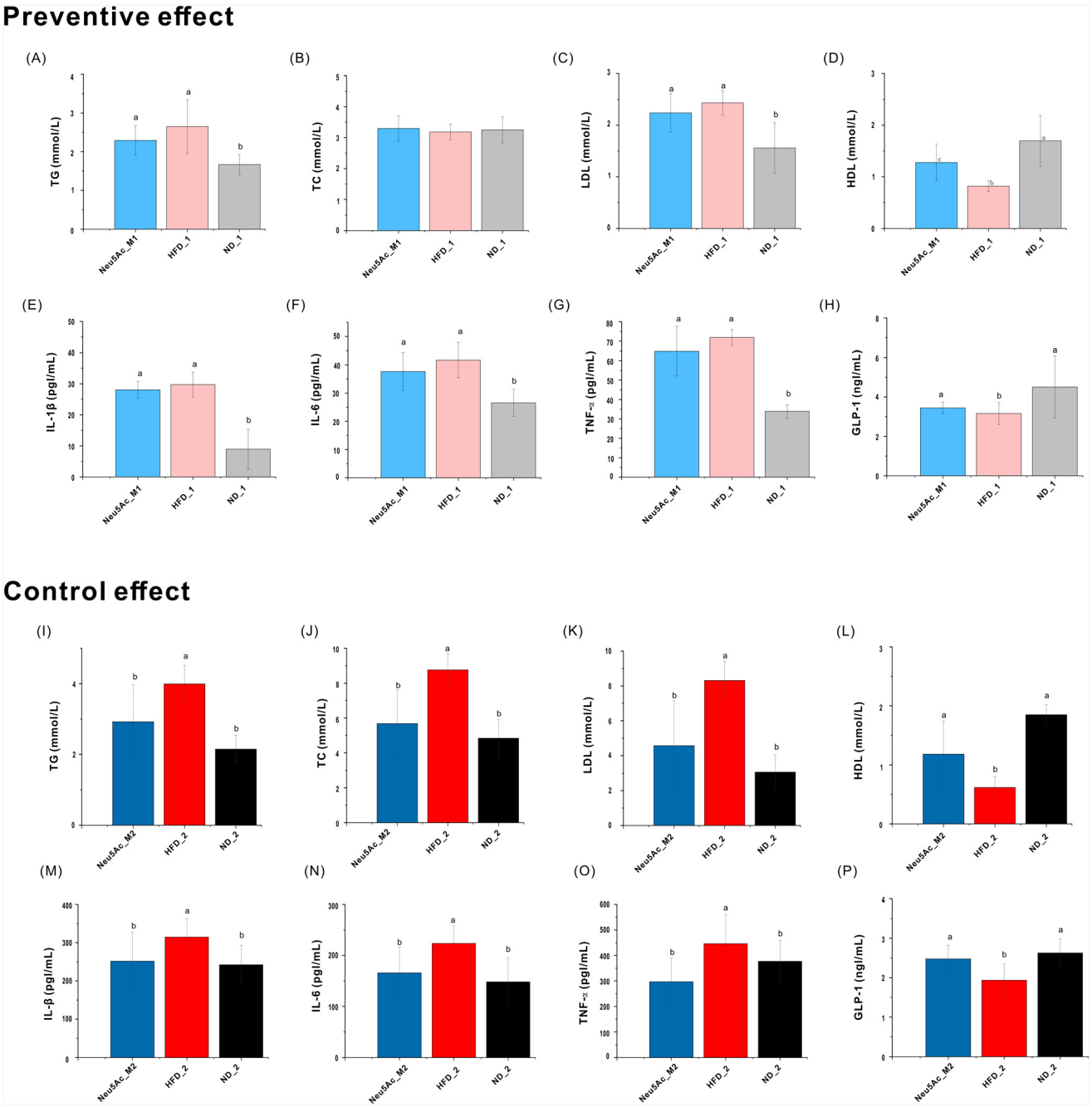

Fig. 4 Effects of *N*-acetylneuraminic acid intervention on blood lipids and serum inflammatory cytokine in high fat-diet mice. (A–H) Preventive experiment: (A) TG (triglycerides); (B) TC (total cholesterol); (C) LDL (low-density lipoprotein); (D) HDL (high-density lipoprotein); (E) IL-1β; (F) IL-6; (G) TNF-α; (H) GLP-1; (I–P) control experiment: (I) TG (triglycerides); (J) TC (total cholesterol); (K) LDL (low-density lipoprotein); (L) HDL (high-density lipoprotein); (M) IL-1β; (N) IL-6; (O) TNF-α; (P) GLP-1.

HFD_2 group (all $P < 0.05$), and serum GLP-1 levels were higher than in the HFD_2 group ($P < 0.05$).

3.5 Gut microbiota

As shown in Fig. 5(A and B), in the prevention experiment: species analysis (phylum level, Fig. 5A): compared with the HFD_1 group, the Neu5Ac_M1 group showed a significant increase in the proportion of *Verrucomicrobiota* and a marked decrease in *Bacteroidota*. Species analysis (genus level, Fig. 5B): in the Neu5Ac_M1 group, the proportions of *Akkermansia* and *Blautia* were significantly higher, while *Faecalibaculum* and *Bacteroides* were significantly reduced compared to the HFD_1 group. Functional analysis [Fig. 5(C–G)]: at level 2, the functional profile of gut microbiota in the Neu5Ac_M1 group followed a similar trend to that of the HFD_1 group. At level 3, Neu5Ac_M1 intervention led to enriched functions associated

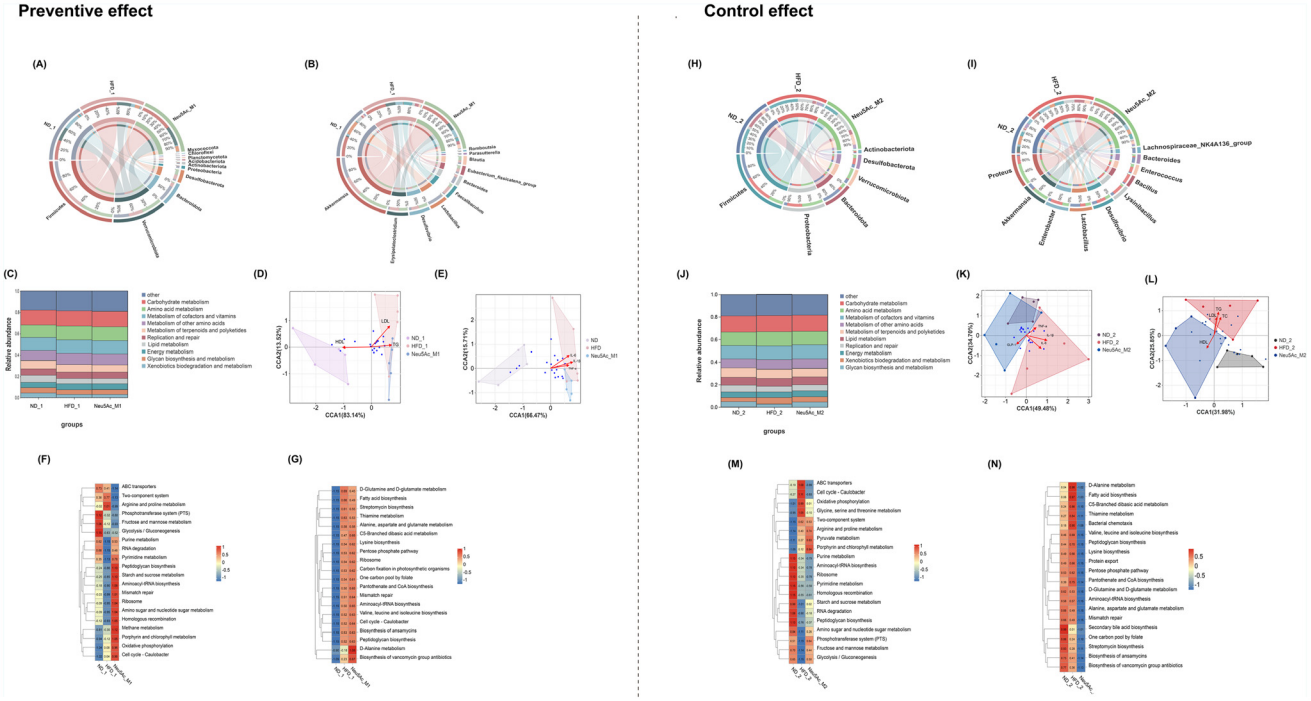

Fig. 5 Effects of *N*-acetylneuraminic acid intervention on gut microbiota in high fat-diet mice. (A–G) Preventive experiment: (A) relative abundance at the phylum level; (B) relative abundance at the genus level; (C) species abundance stacked area plot; (D) canonical correspondence analysis of correlations between serum TC, TG, and HDL with intestinal flora; (E) canonical correspondence analysis of correlations between serum IL-1β, IL-6, and TNF-α with intestinal flora; (F) B-class functional classification of colonic flora based on the PICRUSt2 reference sequence; (G) C-class functional classification of colonic flora based on the PICRUSt2 reference sequence. (H–N) Control experiment: (H) relative abundance at the phylum level; (I) relative abundance at the genus level; (J) species abundance stacked area plot; (K) canonical correspondence analysis of correlations between serum GPL-1, IL-1β, IL-6, and TNF-α with intestinal flora; (L) canonical correspondence analysis of correlations between serum TC, TG, LDL and HDL with intestinal flora; (M) B-class functional classification of colonic flora based on the PICRUSt2 reference sequence; (N) C-class functional classification of colonic flora based on the PICRUSt2 reference sequence.

with Oxidative phosphorylation, ribosome, amino sugar and nucleotide sugar metabolism, mismatch repair, and biosynthesis of vancomycin group antibiotics. These functions are beneficial for gut energy metabolism and maintaining genetic stability. Compared with the ND_1 group, the gut microbiota in the HFD_1 group was associated with elevated blood lipid levels [LDL (Envfit r^2 = 0.44, FDR-adjusted p = 0.028), HDL (Envfit r^2 = 0.74, FDR-adjusted p = 0.003)] and increased serum inflammatory factors [IL-6 (Envfit r^2 = 0.59, FDR-adjusted p = 0.003), IL-1β (Envfit r^2 = 0.56, FDR-adjusted p = 0.012)]. Although the intervention altered the gut microbiota structure, no significant negative correlation was observed between the modified microbiota and the elevated blood lipid/serum inflammatory levels, and the microbiota composition remained distinct from that of the ND_1 group.

As shown in Fig. 5(H–I), in the control experiment: species analysis [phylum level, Fig. 5(H)]: compared with the HFD_2 group, the Neu5Ac_M2 group demonstrated a significant reduction in the proportions of *Firmicutes* and *Desulfobacterota*, while the proportion of *Proteobacteria* increased. Species analysis (genus level, Fig. 5I): the Neu5Ac_M2 group exhibited significantly higher levels of *Akkermansia* and *Proteus*, while the proportions of *Enterobacter* and *Bacillus* were reduced compared to the HFD_2 group. Functional analysis [Fig. 5(J–N)]: at level 2, the Neu5Ac_M2 group showed an opposing trend to the HFD_2 group, with a significant increase in glycan biosynthesis and metabolism and a decrease in xenobiotics biodegradation and metabolism. At level 3, functional microbial abundances related to ribosome, RNA degradation, glycolysis/gluconeogenesis, and peptidoglycan biosynthesis increased. Conversely, functions related to fatty acid biosynthesis and alanine, aspartate, and glutamate metabolism decreased. Furthermore, the alterations in gut microbiota were correlated with serum inflammatory factors [IL-1β (Envfit r^2 = 0.56, FDR-adjusted p = 0.012), IL-6 (Envfit r^2 = 0.45, FDR-adjusted p = 0.033)], suggesting microbiota-mediated regulation of inflammatory pathways [Fig. 5(K)]. The gut microbiota profile of the Neu5Ac_M2 group demonstrated a negative association with hyperlipidemia [TG (Envfit r^2 = 0.65, FDR-adjusted p = 0.004), TC (Envfit r^2 = 0.42, FDR-adjusted p = 0.041)] when compared with the HFD_1 group [Fig. 5(L)].

3.6 Liver and colon transcriptome

As shown in Fig. 6(A–C): the liver transcriptome results of the prevention group revealed that compared to the HFD_1 group,

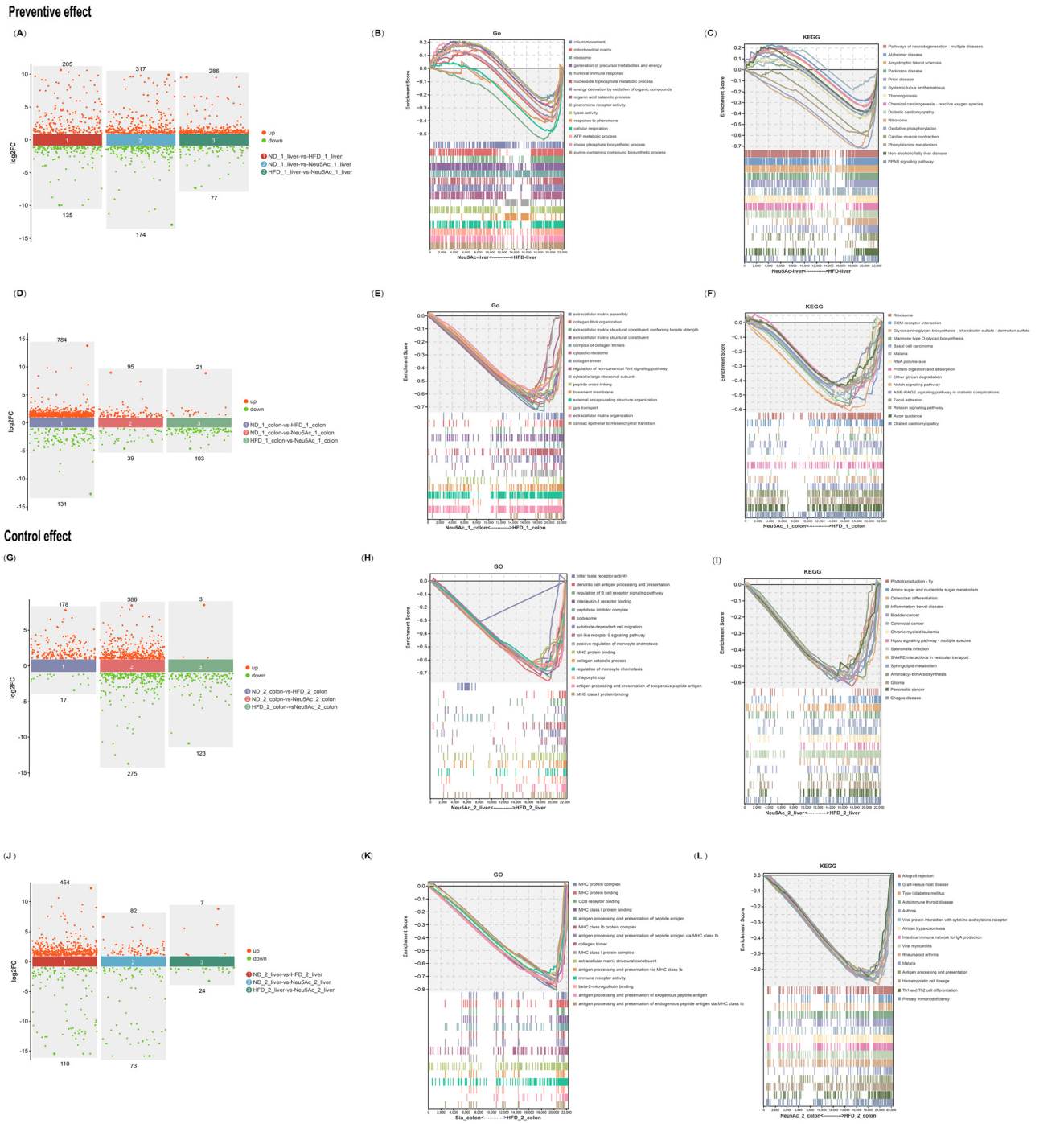

Fig. 6 Effects of *N*-acetylneuraminic acid intervention on liver and colon transcriptome in high fat-diet mice. (A–F) Preventive experiment: (A) scatterplot showing differences in transcript expression levels across multiple groups; (B and C) functional analysis of differential transcriptional expression in the liver (Neu5Ac_1 *vs.* HFD_1 groups): (B) top 15 GO pathways enriched with differentially expressed transcripts between the Neu5Ac_1 and HFD_1 groups; (C) top 15 Kyoto Encyclopedia of Genes and Genomes (KEGG) pathways enriched with differentially expressed transcripts between the Neu5Ac_1 and HFD_1 groups; (D) scatterplot showing differences in transcript expression levels across multiple groups; (E and F) functional analysis of differential transcriptional expression in the colon (Neu5Ac_1 *vs.* HFD_1 groups): (E) top 15 GO pathways enriched with differentially expressed transcripts between the Neu5Ac_1 and HFD_1 groups; (F) top 15 KEGG pathways enriched with differentially expressed transcripts between the Neu5Ac_1 and HFD_1 groups; (G–L) control experiment: (G) scatterplot showing differences in transcript expression levels across multiple groups; (H and I) functional analysis of differential transcriptional expression in the colon (Neu5Ac_2 *vs.* HFD_2 groups): (H) top 15 GO pathways enriched with differentially expressed transcripts between the Neu5Ac_2 and HFD_2 groups; (I) top 15 KEGG pathways enriched with differentially expressed transcripts between the Neu5Ac_2 and HFD_2 groups; (J) scatterplot showing differences in transcript expression levels across multiple groups; (K and L) functional analysis of differential transcriptional expression in the liver (Neu5Ac_2 *vs.* HFD_2 groups); (K) top 15 GO pathways enriched with differentially expressed transcripts between the Neu5Ac_2 and HFD_2 groups; (L) top 15 KEGG pathways enriched with differentially expressed transcripts between the Neu5Ac_2 and HFD_2 groups.

289 differentially expressed genes were upregulated, and 77 were downregulated in the Neu5Ac_M1 group. GASE analysis indicated that the top 15 GO-enriched pathways of these differentially expressed genes were primarily related to energy metabolism, biosynthesis, cell signal transduction, and immune response functions, contributing to the improvement of mitochondrial function and enhanced energy metabolism. The top 15 KEGG-enriched pathways were primarily associated with diseases, immune response, energy metabolism, oxidative stress, and metabolic disorders, indicating an improvement in energy metabolism disorders, oxidative stress, inflammation, and metabolic regulation imbalance. Following the intervention, the Neu5Ac_M1 group exhibited significantly decreased serum levels of AST, ALT, LPS, and OX-LDL compared to the HFD_1 group (all $P < 0.05$), along with improved hepatic architecture and decreased ballooning degeneration [see Fig. 7(A–E)]. These findings suggest that the intervention confers protective effects against oxidative damage and hepatic dysfunction.

As shown in Fig. 6(D–F): the colon transcriptome results of the prevention group showed that compared to the HFD_1 group, 21 differentially expressed genes were upregulated, and 103 were downregulated in the Neu5Ac_M1 group. GASE analysis indicated that the top 15 GO-enriched pathways were mainly related to extracellular matrix (ECM) formation and function, signal transduction, regulation of cell structure and function, as well as tissue development and disease regulation. These findings suggest a reduction in morphological and functional changes in the tissues. The top 15 KEGG-enriched pathways were associated with gene expression, protein synthesis, ECM function, signal transduction, glycosylation, and metabolic regulation. Neu5Ac intervention downregulated pathways related to glucose metabolism and modification, mitigating the impact of a high-fat diet on glucose metabolism, ECM, and signal transduction.

As shown in Fig. 6(G–I): the colon transcriptome results of the control group revealed that compared to the HFD_2 group, 3 differentially expressed genes were upregulated, and 123 were downregulated in the Neu5Ac_M2 group, with fewer differentially expressed genes. GASE analysis showed that the top 15 GO-enriched pathways were primarily involved in immune response, cell signal transduction, antigen processing and presentation, and cell motility and matrix interactions. Neu5Ac intervention reduced colonic immune response and inflammation. The top 15 KEGG-enriched pathways were primarily associated with signal transduction, metabolic regulation, immune response, cancer development, and molecular mechanisms of specific diseases. Neu5Ac intervention downregulated pathological signaling pathways related to bacterial infections, cancer pathways, and intestinal inflammation.

As shown in Fig. 6(J–L): the liver transcriptome results of the control group demonstrated that compared to the HFD_2 group, 7 differentially expressed genes were upregulated, and 24 were downregulated in the Neu5Ac_M2 group. GASE analysis indicated that the top 15 GO-enriched pathways were primarily related to antigen processing and presentation, immune receptor functions, and extracellular matrix structure. Neu5Ac intervention downregulated adaptive immune activation and response pathways. The top 15 KEGG-enriched pathways were mainly associated with immune function regulation and mechanisms of immune-related diseases, showing that Neu5Ac intervention reduced autoimmune damage and improved immune imbalance caused by a high-fat diet. Following the intervention, the Neu5Ac_M2 group showed significantly reduced serum levels of ALT, TMAO, and OX-LDL compared to the HFD_2 group (all $P < 0.05$), along with improved hepatic architecture and decreased lipid vacuolation [see Fig. 7(F–I)]. These results indicate that the intervention exerts protective effects against oxidative damage and liver dysfunction.

4. Discussion

Obesity is an energy balance disorder, primarily characterized by disruptions in glucose and lipid metabolism. This condition is commonly associated with symptoms such as hyperlipidemia and hyperglycemia, posing a significant threat to global health.[35] In this study, we observed that sialic acid intervention had positive effects on lipid and glucose metabolism regulation in both the prevention and control models. Specifically, sialic acid improved glucose tolerance and reduced insulin levels in the mice. Thus, in the high-fat diet model, sialic acid plays a crucial role in addressing the imbalance in glucose and lipid metabolism. The prevention and control experiments revealed different effects between the two models. In the following section, we will discuss how sialic acid intervention prevents obesity in high-fat diet mice and improves glucose and lipid metabolism in obese mice. The goal is to provide insights into the potential effectiveness of sialic acid in addressing glucose and lipid metabolism disorders and, possibly, preventing or controlling obesity.

In this study, compared to the intervention group, the model control mice exhibited a higher rate of weight gain, increased blood lipids, and significantly reduced glucose tolerance. Both experimental groups showed an increase in the abundance of intestinal microbiota associated with energy metabolism and a restructuring of the gut microbiota. Notably, Neu5Ac intervention led to a significant increase in the abundance of *Akkermansia* bacteria, which plays a key role in promoting intestinal mucosal tissue repair through the production of short-chain fatty acids (SCFAs). SCFAs, which serve as substrates for both bacteria and the host, are negatively correlated with inflammatory cytokines and other harmful factors. Additionally, SCFAs can stimulate GLP-1 production, further supporting intestinal barrier function.[36,37] In the prevention group, chronic inflammatory markers did not significantly differ from the model group, and no correlation was observed between these markers and the intestinal microbiota. However, after a longer duration in the control group, a correlation between the reduction in chronic inflammatory markers, the increase in GLP-1 levels, and changes in the gut microbiota was observed.

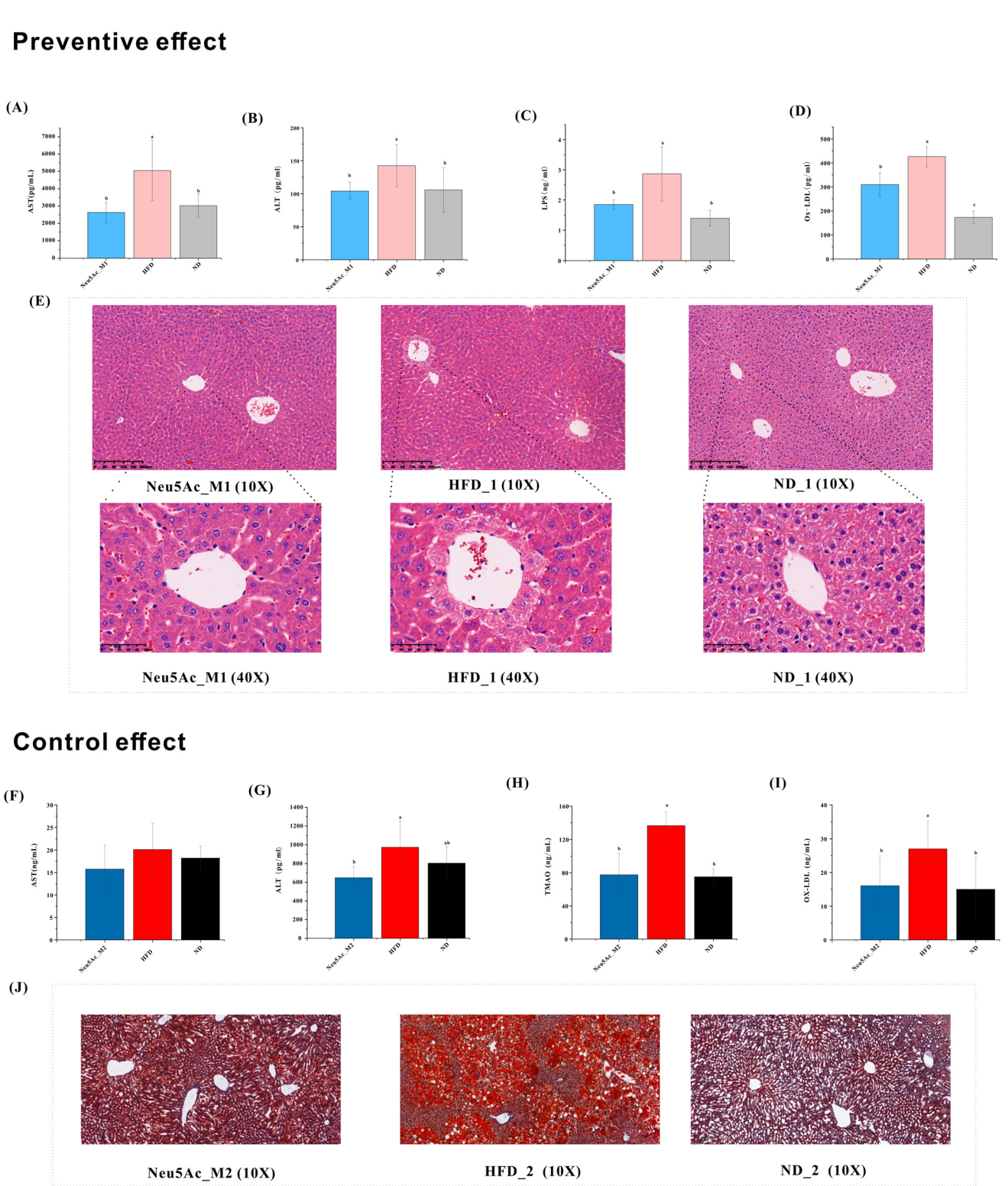

Fig. 7 Effects of *N*-acetylneuraminic acid intervention on hepatic function, pathology, and oxidative stress markers in high fat-diet mice. (A–D) Preventive experiment: (A) AST (Aspartate Aminotransferase); (B) ALT (Alanine Aminotransferase); (C) LPS (Lipopolysaccharide); (D) OX-LDL (Oxidized Low-Density Lipoprotein); (E) hematoxylin and eosin (H&E) staining of liver tissue; (F–J) control experiment: (F) AST (Aspartate Aminotransferase); (G) ALT (Alanine Aminotransferase); (H) TMAO (Trimethylamine *N*-oxide); (I) OX-LDL (Oxidized Low-Density Lipoprotein); (J) oil red O staining of liver tissue.

Transcriptome analysis of the liver and colon revealed that Neu5Ac intervention influenced pathological signaling pathways related to energy metabolism, immune response, and oxidative stress (including chemical carcinogenesis – reactive oxygen species, oxidative phosphorylation, PPAR signaling pathway, and the AGE-RAGE signaling pathway in diabetic complications). Combined with observed reductions in serum oxidative stress markers (OX-LDL and TMAO levels), these findings collectively indicate that the intervention effectively alleviates oxidative stress. Notably, the observed reduction in pro-inflammatory cytokines (*e.g.*, IL-6, TNF-α) further supports the intervention's dual role in mitigating both inflammation and oxidative stress. Studies have shown that the intestinal lamina propria contains a high concentration of both innate and adaptive immune cells.[38,39] High-fat diet-induced intestinal dysbiosis is often accompanied by disruption of the intestinal barrier, alterations in immune cell types, and increased expression of inflammatory cytokines. These changes may exacerbate dysbiosis and promote the development and progression of metabolic diseases. Sialic acid, on the other hand, undergoes extensive modification in the intestinal environment and plays a critical role in host–microbe interactions.[40,41] The homeostasis of intestinal mucus is closely tied to glycosylation, with sialic acid present at the terminal ends of mucin glycans. These sialylated mucins directly interact with intestinal microorganisms. Dietary sialic acid contributes to the body's sialic acid pool, which is integrated into host surface glycans and can provide essential nutrients for intestinal microbiota. Sialylated mucin also protects the mucosal glycoprotein MUC2 from proteolytic degradation by the intestinal flora, thereby maintaining the integrity of the intestinal mucus layer.[42] We hypothesize that Neu5Ac intervention may reduce blood lipids by modulating the gut microbiota, maintaining intestinal barrier homeostasis, mitigating oxidative stress, reducing immune-mediated inflammation through the gut-liver axis, improving insulin sensitivity, and ultimately lowering blood lipid levels.

Notably, our findings revealed that Neu5Ac significantly increased lean mass in HFD-fed mice, despite comparable caloric intake between the HFD and Neu5Ac groups (both higher than the ND group). High-fat diet-induced gut dysbiosis disrupts intestinal barrier integrity, increasing permeability and systemic translocation of bacterial metabolites such as LPS and TMAO. These compounds propagate chronic inflammation through elevated pro-inflammatory cytokines (IL-1, IL-6, TNF-α) and oxidative stress, collectively suppressing muscle protein synthesis while accelerating proteolysis.[43–45] Neu5Ac counteracts these effects through dual mechanisms: restoring gut microbiota homeostasis and enhancing intestinal barrier integrity, while modulating energy metabolism to reduce circulating LPS/TMAO levels. This coordinated action mitigates inflammation and oxidative damage, thereby reversing muscle anabolic suppression and catabolic activation. Collectively, Neu5Ac's multi-target activity synergistically ameliorates HFD-induced metabolic and inflammatory dysregulation *via* the gut-microbiota-metabolism-muscle axis, providing a novel therapeutic avenue for obesity-related metabolic myopathies.

However, we observed differences in both the abundance and function of certain gut microbiota between the prevention and control experiments, particularly regarding the abundance of glycan-modified signal-related microbiota. In the Neu5Ac_M2 control experiment, compared to the prevention experiment, we observed an opposite trend in the intestinal microbiota and the HFD_2 group. Notably, the abundance of functional microbiota involved in processes such as glycolysis/gluconeogenesis and peptidoglycan biosynthesis increased at level 3. Peptidoglycan biosynthesis is crucial for synthesizing peptidoglycan, a major component of the bacterial cell wall. Enhanced biosynthesis of peptidoglycan may indicate an increase in the microbial community's defense capacity or barrier stability,[46] potentially influenced by Neu5Ac. Neu5Ac, a key component of cell surface glycans, is a family of nine-carbon ketone-based acidic monosaccharides and their derivatives, typically found at the distal ends of glycans. It functions as a "bridge" molecule, linking cells to one another and to the extracellular matrix. However, high-fat diets can disrupt the metabolism of Neu5Ac. Studies have shown that a high-fat diet can reduce the sialylation of immunoglobulin IgG, leading to decreased sialylation levels. Hypoglycosylated IgG activates the FcγRIIB receptor on endothelial cells, contributing to obesity-induced insulin resistance.[47] Moreover, glycans on key liver proteins involved in glucose metabolism, such as the insulin receptor (IR) and glucagon receptor (GCGR), are terminally sialylated during glucose metabolism.[48] Additionally, sialyltransferases (STs) mediate Neu5Ac terminal residue modifications in mucins. In terms of glycan chain modification, the control group showed a better intervention effect than the prevention group. In an obese state, sugar chain signaling may undergo significant changes, and Neu5Ac supplementation may help restore normal glycan structure and function. This, in turn, could improve the structure and function of the intestinal microbiota, support immune homeostasis in the intestine and liver, mitigate the inflammatory state, and enhance the body's ability to metabolize glucose and lipids.

We propose that Neu5Ac intake may help alleviate obesity-related pathologies, such as glucose-lipid metabolism disorders induced by high-fat diets. Traditionally, abnormal glucose and lipid metabolism are treated with drugs like statins and metformin. However, due to the complex regulation of glycolipid metabolism, these therapies target only single pathways and carry risks of adverse reactions. Given Neu5Ac' s protective effects on the intestinal barrier and immune system, we suggest that combination therapy, integrating traditional drugs with Neu5Ac, could offer a more effective approach.

5. Conclusion

Neu5Ac interventions have shown a beneficial effect on glucose and lipid metabolism disorders in both the prevention

and control models. However, the effectiveness and underlying mechanisms may differ between the two models. The control group demonstrated a more pronounced effect, likely due to sialic acid's ability to reverse the pathological state of obesity, regulate the intestinal microbiota, modulate immune signaling, and protect glyco-modified states. Future studies should explore the specific molecular mechanisms of sialic acid intervention, particularly its role in improving glycolipid metabolism through the regulation of glycan chain signaling. Additionally, examining the dose–response relationship, individual variability, and interactions with other metabolic regulators of sialic acid will be crucial for advancing this research.

Ethics approval

All experimental procedures were conducted in accordance with the guidelines set by the Institutional Animal Care and Use Committee (IACUC) of the Laboratory Animal Center at Xiamen University, and in compliance with the International Association of Veterinary Editors' guidelines for the Care and Use of Laboratory Animals. The animal use protocol, as detailed below, has been reviewed and approved by the Animal Ethical and Welfare Committee of the Laboratory Animal Center at Xiamen University (Approval No. XMULAC20200185).

Author contributions

All authors contributed to the study conception and design. ZW, HWL, YHL conceived and designed the experiments; ZW, LLZ, XNZ, XYH performed the experiments; ZW, LLZ, XYH analyzed the data; XNZ, HYZ, DBG, XXC, LLP contributed reagents/materials/analysis tools; ZW, LLZ, HWL, YHL wrote the paper. All authors have read and approved the final manuscript.

Data availability

The raw sequencing date from this study have been deposited in the Genome Sequence Archive[49] in BIG Data Center (**https://bigd.big.ac.cn**), Beijing Institute of Genomics (BIG), Chinese Academy of Science, under the accession number: CRA021725 and CRA021834.

Conflicts of interest

The authors declare that they have no competing interests.

References

1 F. Imamura, R. Micha, S. Khatibzadeh, S. Fahimi, P. Shi, J. Powles and D. Mozaffarian, Dietary quality among men and women in 187 countries in 1990 and 2010: a systematic assessment, *Lancet Global Health*, 2015, **3**, e132–e142.
2 A. Więckowska-Gacek, A. Mietelska-Porowska, M. Wydrych and U. Wojda, Western diet as a trigger of Alzheimer's disease: From metabolic syndrome and systemic inflammation to neuroinflammation and neurodegeneration, *Ageing Res. Rev.*, 2021, **70**, 101397.
3 J. Chen, Y. Xiao, D. Li, S. Zhang, Y. Wu, Q. Zhang and W. Bai, New insights into the mechanisms of high-fat diet mediated gut microbiota in chronic diseases, *iMeta*, 2023, **2**, e69.
4 P. J. Turnbaugh, F. Baeckhed, L. Fulton and J. I. Gordon, Diet-induced obesity is linked to marked but reversible alterations in the mouse distal gut microbiome, *Cell Host Microbe*, 2008, **3**, 213–223.
5 H. Wu, W. Zhang, M. Huang, X. Lin and J. Chiou, Prolonged High-Fat Diet Consumption throughout Adulthood in Mice Induced Neurobehavioral Deterioration via Gut-Brain Axis, *Nutrients*, 2023, **15**, 392.
6 J. Dai, D. K. Y. Chan, R. O. Chan, V. Hirani, Y. H. Xu and N. Braidy, The association between dietary patterns, plasma lipid profiles, and inflammatory potential in a vascular dementia cohort, *Aging Med.*, 2023, **6**, 155–162.
7 M. Tencerova, F. Figeac, N. Ditzel, H. Taipaleenmäki, T. K. Nielsen and M. Kassem, High-Fat Diet-Induced Obesity Promotes Expansion of Bone Marrow Adipose Tissue and Impairs Skeletal Stem Cell Functions in Mice, *J. Bone Miner. Res.*, 2018, **33**, 1154–1165.
8 S. S. Ghosh, S. Righi, R. Krieg, L. Kang, D. Carl, J. Wang, H. D. Massey, D. A. Sica, T. W. Gehr and S. Ghosh, High Fat High Cholesterol Diet (Western Diet) Aggravates Atherosclerosis, Hyperglycemia and Renal Failure in Nephrectomized LDL Receptor Knockout Mice: Role of Intestine Derived Lipopolysaccharide, *PLoS One*, 2015, **10**, e0141109.
9 E. Sanguinetti, M. C. Collado, V. G. Marrachelli, D. Monleon, M. Selma-Royo, M. M. Pardo-Tendero, S. Burchielli and P. Iozzo, Microbiome-metabolome signatures in mice genetically prone to develop dementia, fed a normal or fatty diet, *Sci. Rep.*, 2018, **8**, 13.
10 C. J. Chang, C. S. Lin, C. C. Lu, J. Martel, Y. F. Ko, D. M. Ojcius, S. F. Tseng, T. R. Wu, Y. Y. Chen, J. D. Young and H. C. Lai, Ganoderma lucidum reduces obesity in mice by modulating the composition of the gut microbiota, *Nat. Commun.*, 2015, **6**, 7489.
11 F. Siracusa, N. Schaltenberg, Y. Kumar, T. R. Lesker, B. Steglich, T. Liwinski, F. Cortesi, L. Frommann, B. P. Diercks, F. Bönisch, A. W. Fischer, P. Scognamiglio, M. J. Pauly, C. Casar, Y. Cohen, P. Pelczar, T. Agalioti, F. Delfs, A. Worthmann, R. Wahib, B. Jagemann, H. W. Mittrücker, O. Kretz, A. H. Guse, J. R. Izbicki, K. G. Lassen, T. Strowig, M. Schweizer, E. J. Villablanca, E. Elinav, S. Huber, J. Heeren and N. Gagliani, Short-term dietary changes can result in mucosal and systemic immune depression, *Nat. Immunol.*, 2023, **24**, 1473–1486.

12 V. Las Heras, S. Melgar, J. MacSharry and C. G. M. Gahan, The Influence of the Western Diet on Microbiota and Gastrointestinal Immunity, *Annu. Rev. Food Sci. Technol.*, 2022, **13**, 489–512.
13 G. D. Wu, J. Chen, C. Hoffmann, K. Bittinger, Y. Y. Chen, S. A. Keilbaugh, M. Bewtra, D. Knights, W. A. Walters, R. Knight, R. Sinha, E. Gilroy, K. Gupta, R. Baldassano, L. Nessel, H. Li, F. D. Bushman and J. D. Lewis, Linking long-term dietary patterns with gut microbial enterotypes, *Science*, 2011, **334**, 105–108.
14 H. Luck, S. Khan, J. H. Kim, J. K. Copeland, X. S. Revelo, S. Tsai, M. Chakraborty, K. Cheng, Y. Tao Chan, M. K. Nøhr, X. Clemente-Casares, M. C. Perry, M. Ghazarian, H. Lei, Y. H. Lin, B. Coburn, A. Okrainec, T. Jackson, S. Poutanen, H. Gaisano, J. P. Allard, D. S. Guttman, M. E. Conner, S. Winer and D. A. Winer, Gut-associated IgA(+) immune cells regulate obesity-related insulin resistance, *Nat. Commun.*, 2019, **10**, 3650.
15 C. L. Boulangé, A. L. Neves, J. Chilloux, J. K. Nicholson and M. E. Dumas, Impact of the gut microbiota on inflammation, obesity, and metabolic disease, *Genome Med.*, 2016, **8**, 42.
16 M. Yang, X. Qi, N. Li, J. T. Kaifi, S. Chen, A. A. Wheeler, E. T. Kimchi, A. C. Ericsson, R. S. Rector, K. F. Staveley-O'Carroll and G. Li, Western diet contributes to the pathogenesis of non-alcoholic steatohepatitis in male mice via remodeling gut microbiota and increasing production of 2-oleoylglycerol, *Nat. Commun.*, 2023, **14**, 228.
17 Y. Sun, X. Liu, R. Wang, R. Liu, X. Lv, Y. Ma and Q. Li, Lacticaseibacillus rhamnosus HF01 fermented yogurt alleviated high-fat diet-induced obesity and hepatic steatosis via the gut microbiota-butyric acid-hepatic lipid metabolism axis, *Food Funct.*, 2024, **15**, 4475–4489.
18 Y. Wan, F. Wang, J. Yuan, J. Li, D. Jiang, J. Zhang, H. Li, R. Wang, J. Tang, T. Huang, J. Zheng, A. J. Sinclair, J. Mann and D. Li, Effects of dietary fat on gut microbiota and faecal metabolites, and their relationship with cardiometabolic risk factors: a 6-month randomised controlled-feeding trial, *Gut*, 2019, **68**, 1417–1429.
19 I. Z. Pawluczyk, M. G. Najafabadi, J. R. Brown, A. Bevington and P. S. Topham, Sialic acid supplementation ameliorates puromycin aminonucleoside nephrosis in rats, *Lab. Invest.*, 2015, **95**, 1019–1028.
20 J. Lis-Kuberka and M. Orczyk-Pawiłowicz, Sialylated Oligosaccharides and Glycoconjugates of Human Milk. The Impact on Infant and Newborn Protection, Development and Well-Being, *Nutrients*, 2019, **11**, 306.
21 A. Haghani, P. Mehrbod, N. Safi, F. A. Kadir, A. R. Omar and A. Ideris, Edible bird's nest modulate intracellular molecular pathways of influenza A virus infected cells, *BMC Complementary Altern. Med.*, 2017, **17**, 22.
22 K. Nishiyama, A. Nagai, K. Uribayashi, Y. Yamamoto, T. Mukai and N. Okada, Two extracellular sialidases from Bifidobacterium bifidum promote the degradation of sialyl-oligosaccharides and support the growth of Bifidobacterium breve, *Anaerobe*, 2018, **52**, 22–28.
23 M. Huizing, M. E. Hackbarth, D. R. Adams, M. Wasserstein, M. C. Patterson, S. U. Walkley and W. A. Gahl, Free sialic acid storage disorder: Progress and promise, *Neurosci. Lett.*, 2021, **755**, 135896.
24 S. A. Wuensch, R. Y. Huang, J. Ewing, X. Liang and J. T. Lau, Murine B cell differentiation is accompanied by programmed expression of multiple novel beta-galactoside alpha2, 6-sialyltransferase mRNA forms, *Glycobiology*, 2000, **10**, 67–75.
25 R. Zhao, G. Li, X. J. Kong, X. Y. Huang, W. Li, Y. Y. Zeng and X. P. Lai, The improvement effects of edible bird's nest on proliferation and activation of B lymphocyte and its antagonistic effects on immunosuppression induced by cyclophosphamide, *Drug Des., Dev. Ther.*, 2016, **10**, 371–381.
26 X. Yuhan, X. Qiaolin and Z. Wei, Digestion, absorption and utilization of bird's nest salivary acid in rats, *Mod. Food Sci. Technol.*, 2023, **39**(09), 23–32.
27 Z. Yingying, *Study on Kinetics and Monitoring Indexes of Exogenous Sialic acid Intervention*, Master's thesis, Xiamen University, 2020, DOI: 10.27424/d.cnki.gxmdu.2020.000277.
28 M. C. Quek, N. L. Chin, Y. A. Yusof, C. L. Law and S. W. Tan, Characterization of edible bird's nest of different production, species and geographical origins using nutritional composition, physicochemical properties and antioxidant activities, *Food Res. Int.*, 2018, **109**, 35–43.
29 Z. Yida, M. U. Imam, M. Ismail, W. Wong, M. A. Abdullah, A. Ideris and N. Ismail, N-Acetylneuraminic acid attenuates hypercoagulation on high fat diet-induced hyperlipidemic rats, *Food Nutr. Res.*, 2015, **59**, 29046.
30 D. P. Bagchi and O. A. MacDougald, Identification and Dissection of Diverse Mouse Adipose Depots, *J. Visualized Exp.*, 2019, **11**(149), 1–15.
31 D. E. Chusyd, D. Wang, D. M. Huffman and T. R. Nagy, Relationships between Rodent White Adipose Fat Pads and Human White Adipose Fat Depots, *Front. Nutr.*, 2016, **3**, 10.
32 A. Batra, M. M. Heimesaat, S. Bereswill, A. Fischer, R. Glauben, D. Kunkel, A. Scheffold, U. Erben, A. Kühl, C. Loddenkemper, H. A. Lehr, M. Schumann, J. D. Schulzke, M. Zeitz and B. Siegmund, Mesenteric fat—control site for bacterial translocation in colitis?, *Mucosal Immunol.*, 2012, **5**, 580–591.
33 S. Chen, Y. Zhou, Y. Chen and J. Gu, fastp: an ultra-fast all-in-one FASTQ preprocessor, *Bioinformatics*, 2018, **34**, i884–i890.
34 B. Langmead and S. L. Salzberg, Fast gapped-read alignment with Bowtie 2, *Nat. Methods*, 2012, **9**, 357–359.
35 R. A. van der Heijden, F. Sheedfar, M. C. Morrison, P. P. Hommelberg, D. Kor, N. J. Kloosterhuis, N. Gruben, S. A. Youssef, A. de Bruin, M. H. Hofker, R. Kleemann, D. P. Koonen and P. Heeringa, High-fat diet induced obesity primes inflammation in adipose tissue prior to liver in C57BL/6j mice, *Aging*, 2015, **7**, 256–268.
36 B. S. Samuel, A. Shaito, T. Motoike, F. E. Rey, F. Backhed, J. K. Manchester, R. E. Hammer, S. C. Williams, J. Crowley, M. Yanagisawa and J. I. Gordon, Effects of the gut microbiota on host adiposity are modulated by the short-chain

fatty-acid binding G protein-coupled receptor, Gpr41, *Proc. Natl. Acad. Sci. U. S. A.*, 2008, **105**, 16767–16772.

37 H. Ge, X. Li, J. Weiszmann, P. Wang, H. Baribault, J. L. Chen, H. Tian and Y. Li, Activation of G protein-coupled receptor 43 in adipocytes leads to inhibition of lipolysis and suppression of plasma free fatty acids, *Endocrinology*, 2008, **149**, 4519–4526.

38 T. Ogino and K. Takeda, Immunoregulation by antigen-presenting cells in human intestinal lamina propria, *Front. Immunol.*, 2023, **14**, 1138971.

39 A. Montalban-Arques, M. Chaparro, P. G. Javier and D. Bernardo, The Innate Immune System in the Gastrointestinal Tract: Role of Intraepithelial Lymphocytes and Lamina Propria Innate Lymphoid Cells in Intestinal Inflammation, *Inflamm. Bowel Dis.*, 2018, **24**, 1649–1659.

40 O. M. Sokolovskaya, M. W. Tan and D. W. Wolan, Sialic acid diversity in the human gut: Molecular impacts and tools for future discovery, *Curr. Opin. Struct. Biol.*, 2022, **75**, 102397.

41 A. Bell, E. Severi, C. D. Owen, D. Latousakis and N. Juge, Biochemical and structural basis of sialic acid utilization by gut microbes, *J. Biol. Chem.*, 2023, **299**, 102989.

42 K. Bergstrom, X. Shan, D. Casero, A. Batushansky, V. Lagishetty, J. P. Jacobs, C. Hoover, Y. Kondo, B. Shao, L. Gao, W. Zandberg, B. Noyovitz, J. M. McDaniel, D. L. Gibson, S. Pakpour, N. Kazemian, S. McGee, C. W. Houchen, C. V. Rao, T. M. Griffin, J. L. Sonnenburg, R. P. McEver, J. Braun and L. Xia, Proximal colon-derived O-glycosylated mucus encapsulates and modulates the microbiota, *Science*, 2020, **370**, 467–472.

43 Z. Nianyi, W. Fan, L. Junqi, L. Xiang, L. Shaomei, Z. Lang, W. Zhongwei, W. Guangyan, H. Qingfa, Z. Daowen, G. Jie, W. Shan, C. Xiaojiao, C. Muxuan, M. Fanguo, S. Haitao, H. Yan, C. Peng, W. Hong, L. Zhuang and Z. Hongwei, High-fat diet impairs gut barrier through intestinal microbiota-derived reactive oxygen species, *Sci. China:Life Sci.*, 2023, **67**, 879–891.

44 M. Xiaoxing, C. Ruijie, S. Lihui, S. Yunhong, W. Pei, J. Guanhua, W. Lin, L. Xiaoqin, P. Xiaobo, L. Yuxiao, H. Ruikun, Y. Hong and L. Liegang, High-fat diet induces sarcopenic obesity in natural aging rats through the gut–trimethylamine N-oxide–muscle axis, *J. Adv. Res.*, 2025, **70**, 405–422.

45 K. H. Collins, H. A. Paul, D. A. Hart, R. A. Reimer, I. C. Smith, J. L. Rios, R. A. Seerattan and W. Herzog, A High-Fat High-Sucrose Diet Rapidly Alters Muscle Integrity, Inflammation and Gut Microbiota in Male Rats, *Sci. Rep.*, 2016, **6**, 37278.

46 A. J. F. Egan, J. Errington and W. Vollmer, Regulation of peptidoglycan synthesis and remodelling, *Nat. Rev. Microbiol.*, 2020, **18**, 446–460.

47 J. Peng, W. Vongpatanasin, A. Sacharidou, D. Kifer, I. S. Yuhanna, S. Banerjee, K. Tanigaki, O. Polasek, H. Chu, N. C. Sundgren, A. Rohatgi, K. L. Chambliss, G. Lauc, C. Mineo and P. W. Shaul, Supplementation With the Sialic Acid Precursor N-Acetyl-D-Mannosamine Breaks the Link Between Obesity and Hypertension, *Circulation*, 2019, **140**, 2005–2018.

48 J. Peng, L. Yu, L. Huang, V. A. Paschoal, H. Chu, C. O. de Souza, J. V. Varre, D. Y. Oh, J. J. Kohler, X. Xiao, L. Xu, W. L. Holland, P. W. Shaul and C. Mineo, Hepatic sialic acid synthesis modulates glucose homeostasis in both liver and skeletal muscle, *Mol. Metab.*, 2023, **78**, 101812.

49 T. Chen, X. Chen, S. Zhang, J. Zhu, B. Tang, A. Wang, L. Dong, Z. Zhang, C. Yu, Y. Sun, L. Chi, H. Chen, S. Zhai, Y. Sun, L. Lan, X. Zhang, J. Xiao, Y. Bao, Y. Wang, Z. Zhang and W. Zhao, The Genome Sequence Archive Family: Toward Explosive Data Growth and Diverse Data Types, *Genomics, Proteomics Bioinf.*, 2021, **19**, 578–583.